Chemical Engineering Journal 152 (2009) 158–166

Contents lists available at ScienceDirect

Chemical Engineering Journal

journal homepage: www.elsevier.com/locate/cej

A new approach to optimise an annular slurry photoreactor system for the degradation of Congo Red: Statistical analysis and modelling

Meng Nan Chong[a,b], Bo Jin[a,b,c,*], Christopher W.K. Chow[c], Chris P. Saint[c]

[a] School of Chemical Engineering, The University of Adelaide, Adelaide, SA 5005, Australia
[b] School of Earth and Environmental Sciences, The University of Adelaide, Adelaide, SA 5005, Australia
[c] Australian Water Quality Centre, Bolivar, SA Water Corporation, SA 5110, Australia

ARTICLE INFO

Article history:
Received 10 February 2009
Received in revised form 31 March 2009
Accepted 8 April 2009

Keywords:
TiO_2
Congo Red
Annular slurry reactor
Optimisation
Statistical analysis
Design of experiment
Modelling

ABSTRACT

This study utilised design of experiment, and statistical and modelling tools to understand and optimise photodegradation performance of an annular slurry photoreactor (ASP) system using a newly developed titania impregnated kaolinite photocatalyst (TiO_2-K) for the degradation of Congo Red (CR). Using a Taguchi orthogonal array of L_9 $(3)^4$, only 9 experiments were required, instead of 81 experiments in a conventional one-factor-at-a-time approach, to optimise the operational factors of TiO_2-K loading, pH, aeration rate and CR concentration, and to determine their synergistic factor interactions in the ASP system. The apparent first-order rate constants estimated from the Langmuir–Hinshelwood (L–H) model were assigned as the output responses in the designed array. Analysis of variance showed that the CR concentration appears to be the most significant factor, while pH is the least influential on the photodegradation rate. The response surface model with Box–Cox power iterative procedure was used to model the different output responses and determine the synergistic interactions between the system factors. The optimal operating conditions obtained from numerical simulation were regressed to yield an empirical predictive model for modelling the photoactivity in the ASP system. It is anticipated that this statistical model can be used as an effective design tool for scaling up a photocatalytic process for water treatment.

1. Introduction

Since its first inception on the water splitting phenomena in 1972 by Fujishima and Honda, semiconductor photocatalysis utilising titanium dioxide (TiO_2) has attracted tremendous attention across different research fields [1–4]. Water remediation utilising semiconductor TiO_2 first began in 1983 with numerous reported on its efficiency in degrading a wide range of organic contaminants in the aqueous environment [2,4]. The major advantage associated with the use of TiO_2 for organic degradation is the production of carbon dioxide and water as final by-products. Most of the previous researches, however, mainly emphasized on the photodegradation mechanisms of different surrogate organic compounds. To date, modest technical progress was made to develop a photocatalytic technology for an industrial application for water treatment. One of the technical barriers to scale up the photocatalytic technology is the presence of a number of system factors that require rapid coverage testings. In a photocatalytic reactor, system factors include but not limited to the photocatalyst loading, pH, aeration or liquid recirculation rate, concentration of organic contaminants, temperature, light photon flux and intensity and others [3,4].

Previous investigations usually adopted the conventional one-factor-at-a-time approach to optimise the photocatalytic processes, where each operational factor was optimised in sequence [5–8]. In this instance, the applications of the research findings will be restricted. Synergistic interactions between the process operational factors are possible. The desertion made by using the conventional approach might affect the eventual understanding and operation of the process performances. For instance, Chin et al. [7] investigated the effects of pH, aeration rate, TiO_2 and bisphenol-A concentration in batch tests. They found that the optimal factors combination of pH 4, 0.5 g L^{-1} TiO_2 and 0.5 L min^{-1} aeration rate for degrading 10 ppm bisphenol-A. Other factor combinations might have a profound effect on the photodegradation efficiency. In this instance, the synergistic interactions between the process factors can only be determined in a preceding sequence, but not in a random combination. A full coverage testing on the factor interactions through the conventional approach involves the design of a vast number of experiments. If four operational factors are investigated at three different levels, for instance, a complete set of $3^4 = 81$ experiments are required.

* Corresponding author at: School of Earth and Environmental Sciences, The University of Adelaide, Adelaide, SA 5005, Australia. Tel.: +61 8 8303 7056; fax: +61 8 8303 6222.
E-mail address: bo.jin@adelaide.edu.au (B. Jin).

1385-8947/$ – see front matter © 2009 Elsevier B.V. All rights reserved.
doi:10.1016/j.cej.2009.04.027

This paper presents a study using Taguchi design of experiment (DOE) technique and other complementary statistical analyses to optimise an annular slurry photoreactor (ASP) system using a newly developed titania impregnated kaolinite (TiO_2-K) photocatalyst for the degradation of Congo Red (CR). Congo Red is a secondary recalcitrant diazo dye that is commonly found in wastewater and usually can be removed via complex and expensive treatment processes. The highly stable diazo chemical structure, together with its molecular weight and distinct colouring properties make the CR as a surrogate indicator for simulation of ASP system in this study.

In this study, an orthogonal test array design of L_9 $(3)^4$ with 9 standard experiments was used to determine both the most influential and relaxed process operating factors, and the synergistic interactions between the process factors. Four key ASP operational factors, including TiO_2-K loading, water pH, aeration rate and initial CR concentration were employed for the orthogonal array of appropriate order. The apparent first-order rate constants estimated from the Langmuir–Hinshelwood (L–H) kinetic model were used as the output responses in the orthogonal array analysis. Subsequent analysis of variance (ANOVA) was employed to determine the degree of significance for each process factors. The response surface modelling with integrated Box–Cox power iterative procedure was used to reveal best power-transformed response surface model for the representation of output responses obtained. With the aid of a computer simulation, a series of optimum factor combinations was yield and further regressed into a predictive empirical correlation for modelling the ASP system. This statistical-DOE approach is expected to simultaneously reduce the cost and experimentation efforts, and the developed correlation is expected to provide a better understanding and process operation modelling for the development of an industrial photocatalytic process for water treatment.

2. Materials and methods

2.1. Materials

Congo Red ($C_{32}H_{22}N_6Na_2O_6S_2$, Labchem Ajax Finechem, Australia) was manually prepared to the chosen concentrations by the addition of double de-ionised water. Congo Red, a secondary diazo dye, is a recalcitrant azo dye commonly found in wastewater and thus considered to be a representative organic pollutant in wastewater, in terms of its chemical structure, molecular weight and azo bonding. The chemical composition and structure of the Congo Red was described in detail by Chong et al. [9].

The TiO_2-K photocatalyst was successfully developed in our previous study [9]. The TiO_2-K photocatalyst was prepared by the parallel hydrolysis and condensation of titanium (IV) *n*-butoxide, clay heterocoagulation and subsequent firing processing. The exact preparation procedures was proceeded in two-steps before the firing processing, where the titania sol–gel was first produced under a controlled acid-catalysed condition prior to the heterocoagulation with the modified kaolinite clay at 37 °C. Subsequently the firing processing was performed at an increasing heat-flux rate of 2 K/min to 873.15 K. The TiO_2-K photocatalyst was eventually found to exhibit exceptional potential in photoactivity, distinct and stable physical structures, ease of downstream separation and extensive catalyst lifespan [9].

2.2. Annular slurry photoreactor system

A stainless steel-lined ASP column was designed and built for this study. An ultraviolet (UV) light of 11 W (Davis Ultraviolet, Australia) for photonic activation of TiO_2-K photocatalyst was placed annularly inside a quartz thimble to allow effective UV transmission into the reaction zone while preventing the direct contact with the reaction fluid. The ASP column was designed with a detachable conical bottom for free of reaction dead zone, making it easy for cleaning and maintenance. A 45-microns air sparger was fitted to the reactor bottom to provide sufficient aeration and dissolved oxygen by homogeneous bubble distribution. The ASP column has four sampling ports for descending water level sampling and optional base dosing. Measurement probes and meters for in situ data logging of operational pH, dissolved oxygen (DO) and temperature (TPS, Australia) were connected to the reactor during investigation. A detailed design of the ASP system and the whole experimental set up were shown in Fig. 1.

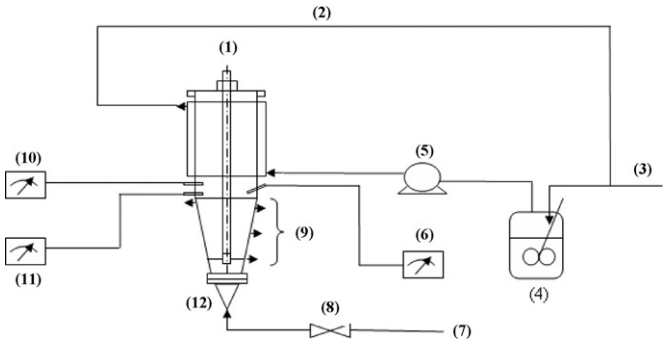

Fig. 1. Experimental set-up for the annular slurry photoreactor system: (1) UV light, (2) recirculation water line, (3) fresh cooling water line, (4) cooling water vessel, (5) cooling water pump, (6) temperature meter, (7) compressed air supply line, (8) compressed air regulation valve, (9) sampling ports, (10) pH meter, (11) dissolved oxygen meter, and (12) photoreactor.

2.3. Experimental setup

Aqueous solution of CR with known concentration was prepared and adjusted to the initial pH value using 2 M hydrochloric acid and 2 M sodium hydroxide, and further verify by the pH meter (TPS, Australia). A relatively low aeration rate was allowed to run through the ASP column to prevent rapid settling of TiO_2-K photocatalyst particles when the TiO_2-K/CR mixture was being introduced. The TiO_2-K/CR mixture was remained bubble in the ASP column for a 0.5 h dark adsorption and stabilisation period prior to UV irradiation at $t = 0$ h. Samples were collected at a 1.0 h interval and centrifugated at 5000 rpm for 10 min for solid TiO_2-K separation. The top supernatant aqueous layer was decanted and filtered using Millex VX filter (Millipore 0.45 μm). The CR concentrations of the filtered samples were measured by an UV–Vis spectrophotometer (Helios Gamma, England) at 496.5 nm. This spectrophotometric concentration measurement technique was proven to correlate well to the extent of mineralisation, expressed in terms of chemical oxygen demand (i.e. mg L^{-1}) in our previous study [10].

2.4. Design and analysis of orthogonal array L_9 $(3)^4$

Orthogonal array (OA) is a statistical DOE that is mostly applied in the manufacturing quality control and rapid software testing for faults detection. It was first functionalised by Dr Genichi Taguchi in the 1950s and known as the Taguchi method, specifically for the cost effective investigation on process optimisation with abundant of systematic factors. Such arrays work in a way, where the effective design of experiments can determine the most influential factor while relaxing the least significant ones. This Taguchi method was eventually carried on to optimise the different factors combination by reducing the variability associated within each chosen combination [11]. When this Taguchi DOE was compared to the conventional one-factor-at-a-time optimisation approach, it was found that the OA-based test runs are uniformly dispersed throughout

the experimental domain, whereas only a small region is covered in the conventional approach. This greatly enhances the identification of factor interactions and variability within the domain, while inversely reducing the time and experimental efforts to achieve similar outcomes.

The OA is a two-dimensional arrays of factors which possess an interesting quality that by choosing any two columns, an even distribution of all pair-wise combinations can be obtained [11]. The followings are some basic terminology employed in the orthogonal arrays [11,12].

- Runs: the number of rows in the orthogonal array and also the number of study cases.
- Factors: the number of columns in the array, which directly translates to the maximum number of variables that can be handled by this array.
- Levels: the maximum number of values that can be taken on by any single factor.
- Strength: the number of columns, i.e. Levels$^{\text{Strength}}$ possibilities.

Thus, the orthogonal array of L_9 $(3)^4$ in this study actually indicated L_{Runs} $(\text{Levels})^{\text{Factors}}$. The different permutations for the chosen factors are fixed, and in this instance all the possible pair-wise factor combinations were shown in Fig. 2. Fig. 2 show the design and analysis of Taguchi OA involved in, four experiment stages of orthogonal design matrix, noise factor matrix, and performance characteristics and statistics. Table 1 summarises the L_9 $(3)^4$ orthogonal array used for this study. After the completion of the array, a parallel noise factor matrix was required for subsequent analysis. When the output responses for the array were defined, each factor combination test run will generate the noise factor combinations based on the value of $\mu \pm \sqrt{3}/2\sigma$, where μ and σ are the mean and standard deviation of the output responses within each test run. With the noise factor matrix, four signal-to-noise (S/N) ratios will be estimated for every test run. Depending on the expected performance statistic of the ASP system, the S/N ratio for every test runs in the orthogonal array can be maximised or minimised. In this instance, the S/N ratio for the ASP system is expected to be "*the larger the better*", where the S/N ratio was maximised according to Eq. (1) for optimum photodegradation rate [11]:

$$S(\kappa) = -10\ \log\left(\frac{1}{n}\sum\frac{1}{K_i^2}\right) \tag{1}$$

2.5. Kinetic model

A rate expression for a single-component heterogeneous photocatalytic reaction that involves the reaction of dye molecules on the surface of a photocatalyst is described by the saturation kinetic expression by Langmuir–Hinshelwood;

$$r = -\frac{d[CR]}{dt} = -\frac{kK_{ads}[CR]}{1 + K_{ads}[CR]} \tag{2}$$

where r is the rate of photodegradation for the dye molecules (mol L^{-1} min^{-1}), k is the rate constant (mol L^{-1} min^{-1}), $[CR]$ is the dye concentration, and K_{ads} is the dynamic Langmuir adsorption constant (M^{-1}). However, there are three assumptions if Eq. (2) is applicable: (i) the reaction system is in dynamic equilibrium; (ii) the reaction is surface mediated, and (iii) the competition for the active surface sites by the intermediates and other reactive oxygen species are not limiting. If all these assumptions are valid, the reaction species in the ASP will only consist of the adsorption surface sites, dye molecules and its intermediates, the electron-hole pairs and the reactive oxygen species. The rate constant, k interprets as the intrinsic reaction rate constant. This includes the rate of $OH^{\bullet}$ and $O_2^{\bullet -}$ generation, a function of the absorbed photon flux, I_{abs} $[O_2]_{ads}$, competition from intermediate products, and mass transport effects. The Langmuir saturation term $K_{ads}[CR]/(1 + [CR])$ in Eq. (2) represents the fraction of surface sites occupied by the dye molecules.

The implicit solution for Eq. (2) is given as in Eq. (3);

$$\ln\left(\frac{[CR]}{[CR]_0}\right) + K_{ads}([CR] - [CR]_0) = -kK_{ads}t \tag{3}$$

which can be solved explicitly for t by using discrete change in the dye concentration $[CR]$ from initial concentration to a zero point of reference.

Eq. (3) can be applied to yield the exact solution for the photodegradation of CR. When the CR concentration is low (i.e. in milimoles), an apparent first order model (Eq. (4)) can usually be assumed by combining both the rate constant k with the Langmuir adsorption constant K_{ads} to yield the apparent rate constant term, k' (min^{-1}).

$$r = -\frac{d[CR]}{dt} = kK_{ads}[CR] = k'[CR] \tag{4}$$

Rearranging and integration of Eq. (4) yields the pseudo-first order model in Eqs. (5) and (6) and such models have been applied in several photocatalysis studies to characterise the effects of different experimental conditions on the photodegradation rate.

$$[CR] = [CR]_0 e^{-k't} \tag{5}$$

$$\ln\left(\frac{[CR]_0}{[CR]}\right) = -kK_{ads}t = -k't \tag{6}$$

To evaluate the k and K_{ads}, a plot of the reaction rate at different CR concentrations can be carried out. An equivalent expression for the L–H model that can be applied for such evaluation is shown in Eq. (7), where both k and K_{ads} can be obtained from the intercept and slope of the line formed when $1/r_0$ is plotted against $1/[CR]_0$

$$\frac{1}{r_0} = \frac{1}{k} + \frac{1}{kK_{ads}[CR]_0} \tag{7}$$

3. Results and discussion

3.1. Determination of apparent first order rate constant

The principal interest using Taguchi array is to determine the optimal operational factors and their combinations, and to identify the most influential factors on the CR degradation rate. Table 1 shows the L_9 $(3)^4$ orthogonal array design for this study. Table 1 presents the distinct characteristic of the array in which each chosen factor was combined in a pair-wise permutation without repeating itself in any other combinations. Each factor combinations, however, required an output response to convey the variability effects between every factor combination. The photodegradation profiles exhibited a surface saturation kinetic prototype, where an equilibrated dye concentration–time profile was reached. The apparent first order reaction rate (k') from the L–H model was applied as the output response for the array.

Since the k and K_{ads} were unknown, a graphical estimation was required prior to the determination of the k'. The k and K_{ads} could be then estimated from the intercept and slope of the reciprocal plot of CR photodegradation rate against the CR concentrations, respectively. From the 9 array test runs, the initial rate (r_0) was found to be in the range of 7.15×10^{-8} to 2.14×10^{-7} mol L^{-1} min^{-1}, with initial CR concentrations of 2.70×10^{-5} to 8.89×10^{-5} mol L^{-1}. Fig. 3 shows the L–H fitted kinetic profiles for each test runs with the inset being the plot of $1/r_0$ against $1/[CR]$. The k was calculated as 4.12×10^{-6} mol L^{-1} min^{-1} as the K_{ads} varied from 2.55×10^3 L mol^{-1} to 8.40×10^3 L mol^{-1}. Thus the k' for each test run was determined to be in the range of 1.05×10^{-2} min^{-1} to 3.46×10^{-2} min^{-1}. These

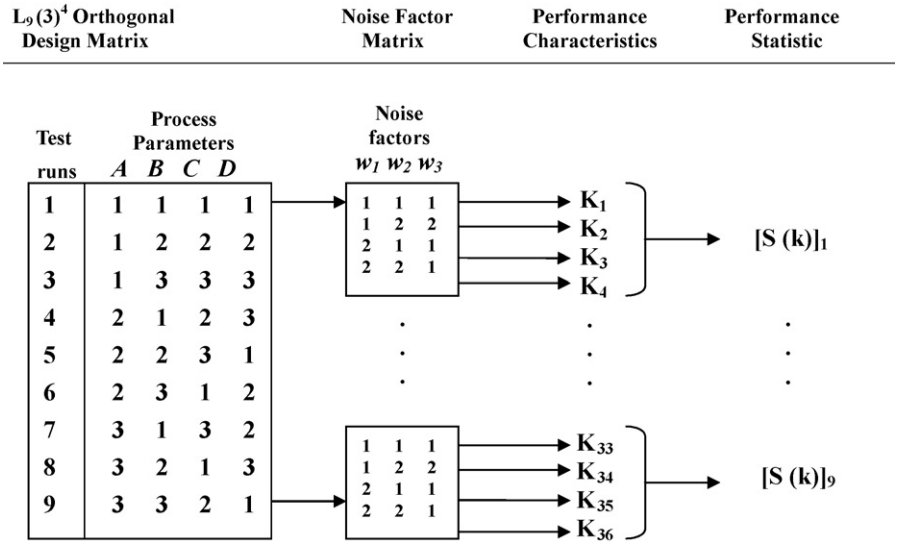

Fig. 2. L_9 $(3)^4$ Taguchi orthogonal array design of experiment and the associated interpretation and analysis flow diagram.

Table 1
The L_9 $(3)^4$ orthogonal array design for the optimisation of factors influencing the photodegradation of Congo Red in the APR system.

Test no. (matrix)	Factors								Output response
	(A)	TiO_2-K (g/dm^3)	(B)	pH	(C)	Aeration rate (dm^3/min)	(D)	CR concentration (mg/dm^3)	S_i
1	A1	4	B1	5.0	C1	5	D1	20	0.0112
2	A1	4	B2	7.0	C2	7.5	D2	40	0.0242
3	A1	4	B3	10.0	C3	10	D3	60	0.0346
4	A2	6	B1	5.0	C2	7.5	D3	60	0.0329
5	A2	6	B2	7.0	C3	10	D1	20	0.0105
6	A2	6	B3	10.0	C1	5	D2	40	0.0240
7	A3	8	B1	5.0	C3	10	D2	40	0.0240
8	A3	8	B2	7.0	C1	5	D3	60	0.0317
9	A3	8	B3	10.0	C2	7.5	D1	20	0.0110

values were assigned as the output responses for each of the Taguchi array test run as discussed in Section 3.2. Therefore, the optimum operating factor level and their combinations within the four factors of TiO_2-K loading, pH, aeration rate and initial CR concentration were determined at three different levels in the ASP system.

3.2. Interpretation of Taguchi array and analysis of variance (ANOVA)

Since the L–H apparent first order reaction rate constants were used as the output responses for the L_9 $(3)^4$ orthogonal arrays, the

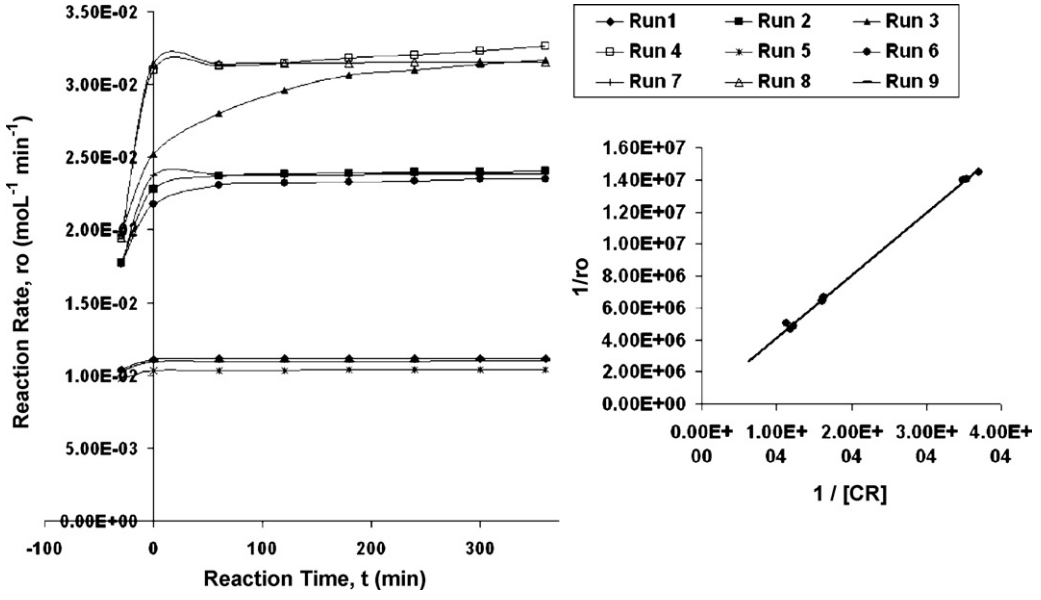

Fig. 3. Langmuir–Hinshelwood profiles for the Taguchi OA standard test runs. (Inset: plot of $1/r_0$ against $1/[CR]$.)

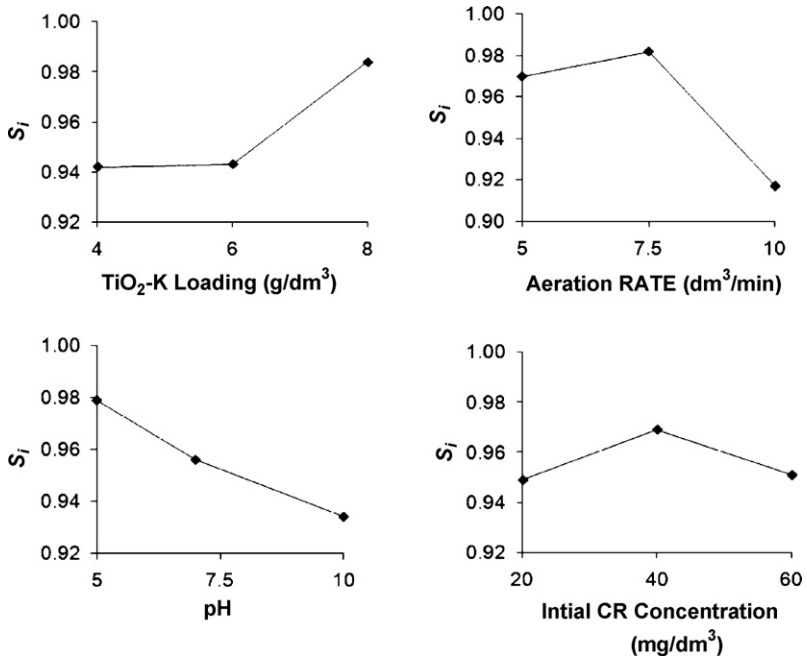

Fig. 4. Effects of TiO_2-K loading, pH, aeration rate and initial CR concentration on the photodegradation rate of CR in APR.

optimal operating factors and their combinations in the ASP can be determined. The statistic values of *S*, designated as S_1 to S_9 have been permuted according to the Taguchi analysis (Fig. 4) [11–13]. These *S*-values represent the *S*/*N* ratio of Taguchi analysis, where the signal corresponds to the photodegradation rate in the ASP through the k'-values interpretation and noise refers to other systematic factors. These systematic factors might deviate the actual output responses from their average nominal values. Fig. 4 shows the relative *S*-values against each operational factor of TiO_2-K loading, pH, aeration rate and initial CR concentrations. It can be concluded that the factor combination at its corresponding optimal levels were $A_3B_1C_2D_2$. These indicate that the optimal operating conditions for the photodegradation of 40 ppm (D_2) of CR occurred at TiO_2-K loading 8 g dm^3 (A_3), pH 5 (B_1) and aeration rate of 7.5 dm^3 min^{-1} (C_2).

We used analysis of variance (ANOVA) on the output *S*/*N* ratio associated with every test run to identify the distinct characteristic between the control or signal factors. Control factors are factors that give a more significant effects on the *S*/*N* ratio, while the signal factors is the one with the smallest effect and usually can be relaxed [14]. In order to achieve a better control of the variability, the *S*/*N* ratio was maximised according to Eq. (1), to yield a high photodegradation rate [15]. Since the variability is inversely proportional to the *S*/*N* ratio, the experiment with maximum *S*/*N* ratio is thus considered as optimum.

This study also employed different response surface models to evaluate their suitability in simulating the output responses for the CR photodegradation in the ASP system [16]. The general form of the polynomial model and its related coefficients were calculated using Eq. (8):

$$Y = b_0 + \sum_{i=1}^{N} b_i X_i + \sum_{i=1}^{N} b_{ij} X_i^2 + \sum_{i_{i<j}}^{N} \sum_{j}^{N} b_{ij} X_i X_j \quad (8)$$

where *Y* was the predicted output responses of the L–H apparent first order rate constant (min^{-1}), and *i*, *j* were linear, quadratic coefficients, respectively. In this instance, the signal factors were made as the linear term while the noise factors were the quadratic terms. The parameters of *b* and *N* were regression coefficient and the number of factors studied in the experiment, respectively.

Statistical results from the response surface simulations showed that the output responses can be best represented by the linear form of response surface model. The Fisher's *F*-distribution test on the output responses resulted in an *F*-value of 74.16, which indicated that the linear terms is more significant compared to any other response surface models. From Table 2, the *p*-value for the linear model was estimated to be 0.005. This implies that there was only a 0.05% chance that the linear model *F*-value can occur in this study. Furthermore, the predicted R^2 values using different response surface models were compared with their adjusted R^2 values for model accuracy. It was found that the predicted R^2 value of 0.9346 for the linear model gives the most reliable approximation to the adjusted R^2 value of 0.9734. Since the significance of the *F*-value was tested in the addition of linear terms to the intercept and block effects, a small *p*-value (Probability > *F*) actually indicates that the addition of interaction terms can improve the model. When the 2-factor interaction was evaluated, however, it was found that its addition to the linear terms does not improve the significance of the model used. The *F*-value decreased to 66.22, with *p*-value of 0.0943 when the interaction terms were accounted. Among the possible interaction terms from the Taguchi DOE in this study, it was found that the TiO_2-K loading (A) has a positive synergistic effects when being coupled with the aeration rate (C) only. Detrimental effects on the overall DOE output responses were generated by other possible interaction terms between TiO_2-K loading with pH (AB) and pH with aeration rate (BC). Fig. 5 shows the interaction between the studied factors. All these prove that the linear response surface model can be used to simulate the output responses. All the subsequent ANOVA analyses were based on the linear model.

Table 2 shows the estimated results from the ANOVA on the output responses in this study. Apart from the *S*/*N* ratio of the ASP system, ANOVA can also be used to identify which factors would significantly affect the quality characteristic of the output responses or which factors that can be relaxed. Specifically, the operational factors that significantly affect the photodegradation rate in the ASP system can be numerically compared. In Table 2, the term SS represents the sum of square for each factor, df is the degree of freedom,

Table 2
ANOVA for Taguchi OA output responses using linear response surface model.

ANOVA for response surface linear model					
Source	Sum of squares (SS)	df	Mean square (MS)	*F*-value	*p*-value Prob > *F*
Model	7.42E−04	4	1.85E−04	74.16	0.0005
A-TiO_2-K loading	1.78E−06	1	1.78E−06	0.7129	0.4460
B-pH	5.36E−07	1	5.36E−07	0.2144	0.6674
C-aeration rate	8.66E−07	1	8.66E−07	0.3465	0.5877
D-initial [*CR*]	7.38E−04	1	7.38E−04	295.37	<0.0001
Residual	1.00E−05	4	2.50E−06		
Correlation total	7.52E−04	8			

and MS is the mean square for each factor. The *F*-value for factor *D* (CR concentration) was found to be the highest, with value of $F_D = 295.37$ and $p < 0.0001$. This indicated that any changes in the initial CR concentration will lead to the most significant influence on the CR degradation rate. The *F*-values for other factors of TiO_2-K loading (F_A), pH (F_B) and aeration rate (F_C) were also estimated. It was found that the *F*-values for F_A, F_B and F_C were quite insignificant, corresponding to *p*-values of 0.4460, 0.6674 and 0.5877, respectively. The method of pooling for insignificant factors to an error term is usually applied when the degree of freedom is low [14,15]. However, this was found to be redundant in this case. From all the estimated *F*-values, it can be concluded that the sequence of factor influence on a descending rank for each of the studied factors was *D* > *A* > *C* > *B*.

Further statistical analyses were performed to determine the predictive accuracy of the linear response surface model in the interpretation of the output responses. Fig. 6a shows the normal plot of residuals, where the normal percentage of probability was plotted against the internally studentized residuals (ISR). These residuals are the number of standard deviations that separate the actual and predicted output responses, and can be estimated from the residual divided by the estimated standard deviation of the residual [17]. Thus, this normal plot indicates whether the residuals will follow a normal distribution, which is a straight line in this case. It can be seen that the estimated ISR from the output responses approximately fitted to a straight line. Another plot for the model prediction against the actual output responses (Fig. 7a) indicate that the linear response surface model can be described very well as a straight line. Furthermore, a conventional Box–Cox (B–C) power plot was graphed (Fig. 8) to determine the most appropriate power transformation to idealise the slight deviation between the model prediction and actual output responses [18]. Most power transformation function can be described by the standard equation of $\sigma = \text{function}(\mu^{\alpha})$, where σ is the standard deviation, μ is the mean, α is the power, and λ is $(1-\alpha)$ in all cases [18]. The power origin of the linear response surface model has unity power transformation with $\lambda = 1$. From Fig. 8, the minimum point in the B–C plot represents the λ value, resulting in a minimal residual sum of squares for the corresponding output responses. The λ-values at 95% confidence interval for the current power transformation could be calculated from the, B–C plot in order to determine the acceptable range of λ-values for the current output responses. Results showed that the

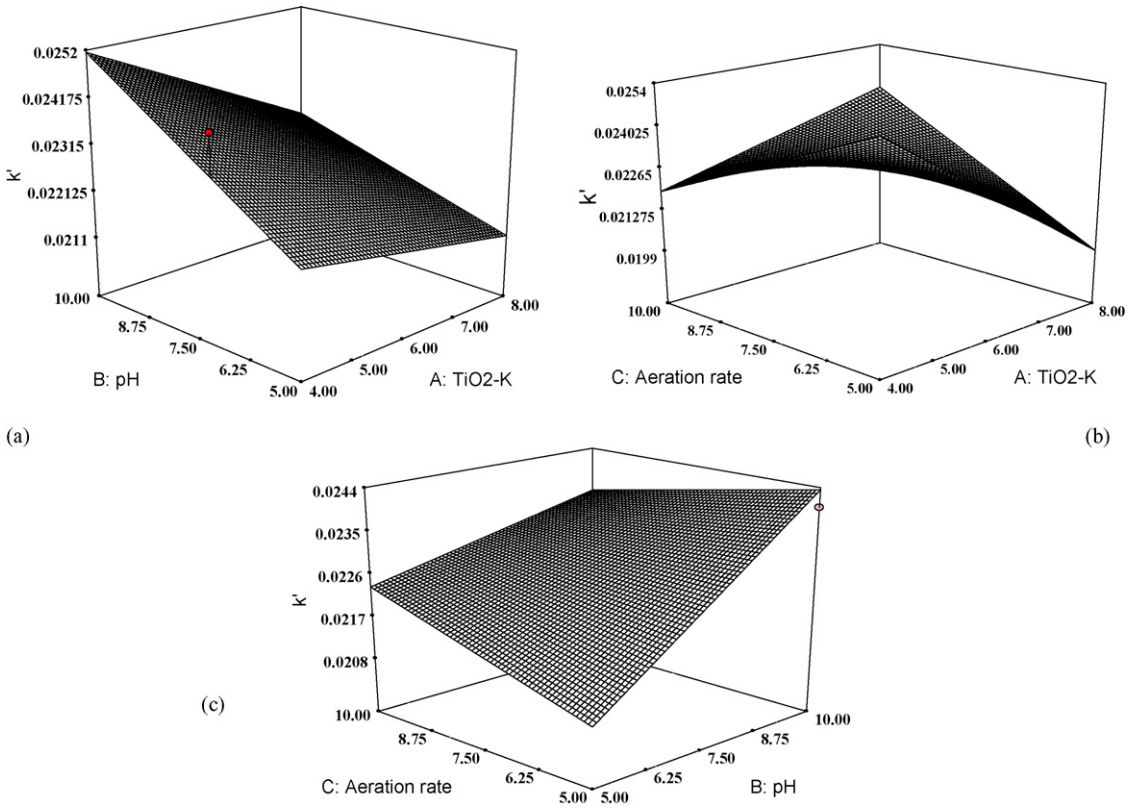

Fig. 5. Response surface plots for 2-factor interaction during the photodegradation of CR in the ASP; (a) TiO_2-K: pH; (b) TiO_2-K: aeration rate; (c) pH: aeration rate.

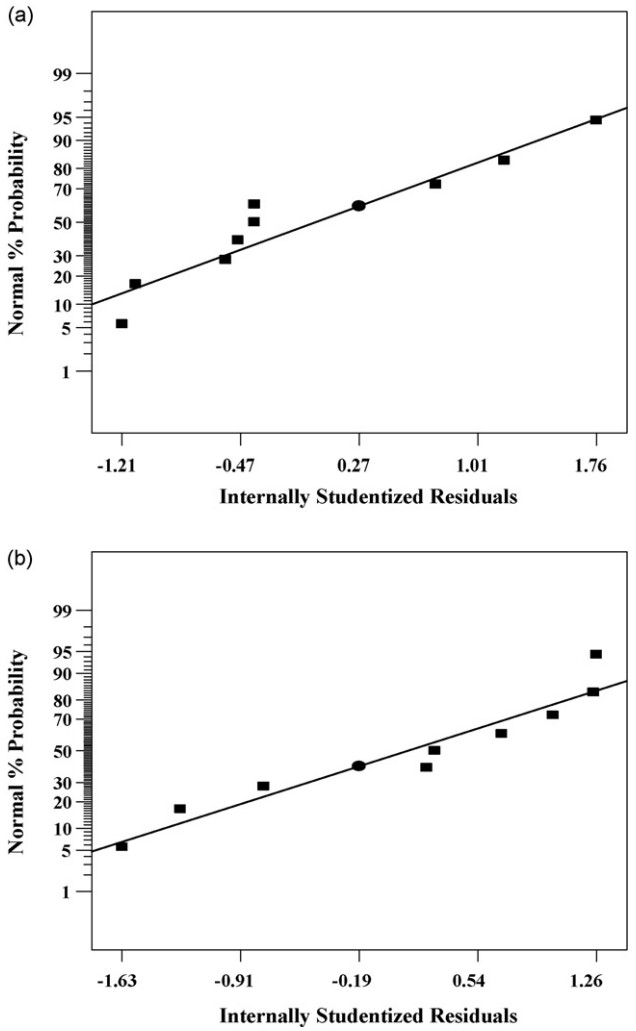

Fig. 6. Plot of normal % probability against internally studentized residuals. (a) $\lambda = 1$; (b) $\lambda = 1.72$.

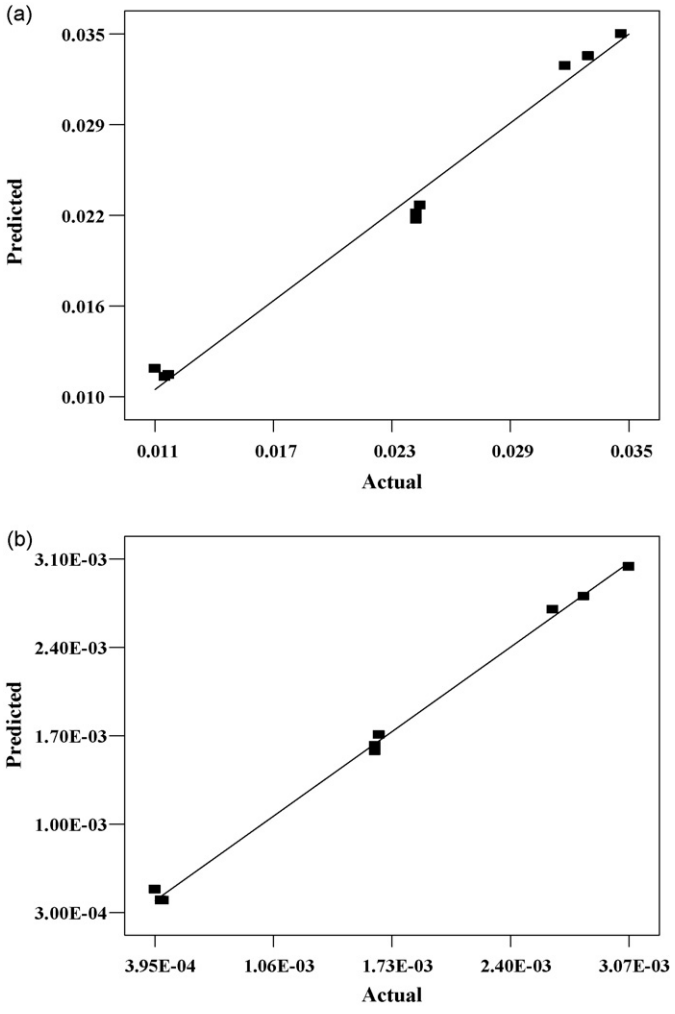

Fig. 7. Plot of predicted versus actual value of response outputs (prediction model = linear response surface model) (i) $\lambda = 1$; (ii) $\lambda = 1.72$.

95% confidence interval for $\lambda = 1.27–2.16$, with optimal power transformation at $\lambda = 1.72$. This implies that a 1.72-power transformed linear response surface model can perfectly interpret the output responses of the Taguchi OA for optimal *S*/*N* ratio. Therefore, a comparison was made to evaluate the differences for the ANOVA outcomes at $\lambda = 1$ and 1.72, respectively.

Table 3 shows the ANOVA and other statistical analyses outcomes when the λ is power-transformed by the value of 1.72. When the *F*-values for both $\lambda = 1$ and 1.72 was compared, the power transformed model yielded a statistically significant result with an *F*-value enhancement factor of 5-folds. The *p*-value of the transformed model further validated its application reliability with a value of 0.0001%, indicating that the entire Taguchi DOE used has 0.0001% chance that it will be affected by the noise factors. The appropriateness of the power transformed model can also be found from the small deviation between the predicted R^2 values to the adjusted R^2 value as shown in Table 3. Other comparisons can also

Table 3
Comparison for power transformed response surface model with different λ-values.

Summary	$\lambda = 1$	$\lambda = 1.72$
Model *F*-value	74.16	419.78
p-value (Prob > *F*)	0.0005	<0.0001
Standard deviation	1.58E−03	7.27E−05
Mean	2.27E−02	1.64E−03
C.V. %	6.97	4.45
PRESS	4.91E−05	1.40E−07
R^2	0.9867	0.9976
Adjusted R^2	0.9734	0.9952
Predicted R^2	0.9346	0.9842
S/*N* ratio	20.07	48.80

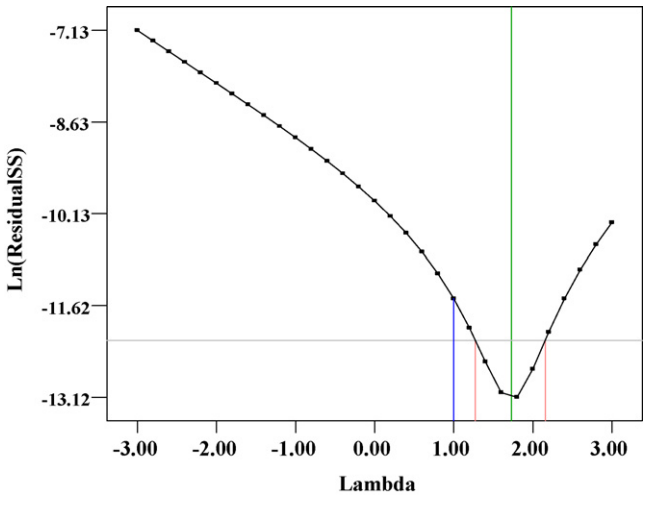

Fig. 8. Box–Cox plot for output responses using linear response surface model.

be made from both Figs. 6b and 7b with its predecessor when λ was transformed to 1.72. Further proof comes from the *S*/*N* ratio, where the significantly high *S*/*N* ratio from the power transformed model indicated an adequate model signal to navigate the current study domain. It should be noted that for the power transformed model, the λ changes do not affect the Taguchi analyses and can only provide a more reliable model for data support and interpretation, and its subsequent optimality study.

3.3. Comparisons of Taguchi method with conventional method

Previous studies using the conventional one-factor-at-a-time approach rarely investigated the factors interaction and its simultaneous operational level change during the process optimisation. An optimum sequenced factor combination was usually yielded after a series of 12 experiments with no knowledge on the random pair-wise factor interactions. From our previous study, the optimal factor combination using conventional optimisation approach with the same experimental domain was found to be TiO_2-K loading of 6 g dm^3 at pH < 9.5, aeration rate of 7.5 dm^3 min^{-1} and initial CR concentration of 40 ppm [19]. This optimal factor combination, however, is impractical for a large-scale operation as it does not convey useful information when any of the studied factors are varied in a random manner.

With the aid of Design Expert® 7.1.3 software, a series of optimal factor combinations was obtained from the computer-aided simulation. A substantial set of 39 optimal factor combinations were yielded to maximise the L–H apparent first order rate constant for the CR photodegradation in the ASP system. From the 39 optimal solutions, 19 combinations have unity desirability. The set of optimal solutions together with their corresponding factor levels, predicted L–H apparent first order rate constant and desirability (i.e. possibility to occur) were calculated. It was observed that an optimal solution could not be found out when all of the studied factors were sequentially determined to be optimum. Other factor combinations were possible, when one factor offsets another during the randomized operational level change. With these optimal combinations, an empirical correlation model was established using multiple regression analysis to predict the ASP operational performance within the study domain (i.e. Eq. (9)) [20].

$$Y_{k'} = 1.13 \times 10^{-4} - 2.73 \times 10^{-4}(\mathrm{TiO_2\text{-}K\ Loading}) + 1.19 \times 10^{-4}(\mathrm{pH}) + 1.52 \times 10^{-4}(\mathrm{Aeration\ Rate}) + 5.55 \times 10^{-4}(\mathrm{Initial\ CR\ Concentration}) \quad (9)$$

If the constraints for the study domain were found to be inadequate to obtain a new design scope, the proposed study can be expanded and repeated using the proposed statistical methods to achieve a better accuracy. The robustness of such statistical methods can also be expanded to incorporate with the water qualities by introducing a fractional correction factor, and taking the photodegradation of single component, such as CR, as the base case. Using these statistical methods, a robust combinatorial optimisation approach could be introduced to optimise and model TiO_2 photocatalysis process.

4. Conclusion

This work has demonstrated a new approach to use efficient DOE and other complementary statistical methods to successfully identify the optimal factor combinations and their interactions within the ASP system. As a result of Taguchi interpretation, the maximum photodegradation rate of CR could be achieved under the optimised operation conditions with TiO_2-K loading of 8 g dm^3 and initial CR concentration of 40 mg dm^3 at pH 5 and aeration rate of 7.5 dm^3 min^{-1}. From ANOVA, the initial CR concentration was found to be the most significant factor that affects the overall photocatalytic performance within the ASP system, followed by TiO_2-K loading and aeration rate. The pH variation in the range of 5–10 appeared to have less significant impact on the photodegradation rate. It was also found that the addition of factor interaction terms to the linear response surface model does not improve the significance of the model. Conversely the accuracy of the linear response surface model could be enhanced from a λ-power transformed of 1.72/1.00. With this DOE-statistical approach, a multiple factor combinations were obtained through the computer-aided numerical simulation. These factor combinations could provide a useful approach to comparison and standardisation of similar studies, and an insight into optimisation and modelling of the ASP system.

The statistical model developed in this study can be further expanded to incorporate different water sources and TiO_2 photocatalysts used. Application of this combined DOE and statistical methods is found to be not only time effective but a useful tool to determine the interactions between all operational factors, level optimality, sensitivity analysis, and to provide an empirical statistical modelling. This study introduced a relatively new approach for optimisation and predictive modelling of a TiO_2 photocatalytic process for water treatment.

Acknowledgements

This work was supported by the Australian Research Council Linkage Grant (LP0562153) and Australian Water Quality Centre, SA Water Corporation through the Water Environmental Biotechnology Laboratory (WEBL) at the University of Adelaide.

References

[1] A. Fujishima, K. Honda, Electrochemical photolysis of water at a semiconductor electrode, Nature 238 (1972) 37.
[2] K. Pirkanniemi, M. Sillanpaa, Heterogeneous water phase catalysis as an environmental application: a review, Chemosphere 48 (2002) 1047.
[3] D. Bahnemann, Photocatalytic water treatment: solar energy applications, Solar Energy 77 (2004) 445.
[4] U.I. Gaya, A.H. Abdullah, Heterogeneous photocatalytic degradation of organic contaminants over titanium dioxide: a review of fundamentals, progress and problems, J. Photochem. Photobiol. C: Photochem. Rev. 9 (2008) 1.
[5] A. Bhargava, M.F. Kabir, E. Vaisman, C.H. Langford, A. Kantzas, Novel technique to characterize the hydrodynamics and analyse the performance of a fluidized-bed photocatalytic reactor for wastewater treatment, Ind. Eng. Chem. Res. 43 (2004) 980.
[6] A.P. Toor, A. Verma, C.K. Jotshi, P.K. Bajpai, V. Singh, Photocatalytic degradation of Direct Yellow 12 dye using UV/TiO_2 in a shallow pond slurry reactor, Dyes Pigments 68 (2006) 53.
[7] S.S. Chin, T.M. Lim, K. Chiang, A.G. Fane, Factors affecting the performance of a low-pressure submerged membrane photocatalytic reactor, Chem. Eng. J. 130 (2007) 53.
[8] I.J. Ochuma, R.P. Fishwick, J. Wood, J.M. Winterbottom, Optimisation of degradation conditions of 1,8-diazabicyclo[5.4.0]undec-7-ene in water and reaction kinetics analysis using a cocurrent downflow contactor photocatalytic reactor, Appl. Catal. B: Env. 73 (2007) 259.
[9] M.N. Chong, V. Vimonses, S. Lei, B. Jin, C. Saint, C. Chow, Synthesis and characterisation of novel titania impregnated kaolinite nano-photocatalyst, Micro. Meso. Mater. 117 (2009) 233.
[10] M.N. Chong, B. Jin, H.Y. Zhu, C. Chow, C. Saint, Application of H-titanate nanofibers for degradation of Congo Red in an annular slurry photoreactor, Chem. Eng. J. 150 (2009) 49.
[11] G. Taguchi, System of Experimental Design, Vols. 1 and 2, UNIPUB Krauss International, New York, 1987.
[12] Z. Li, O.P. Malik, An orthogonal test approach based control parameter optimization and its application to a hydro-turbine governor, in: 199 IEEE Trans. on Energy Conver., vol. 12, 1997, p. 388.
[13] W. Charteris, Taguchi's system of experimental design and data analysis: a quality engineering technology for the food industry, J. Soc. Dairy Technol. 45 (1992) 33.
[14] K.D. Kim, S.H. Kim, H.T. Kim, Applying the Taguchi method to the optimization for the synthesis of TiO_2 nanoparticles by hydrolysis of TEOT in micelles, Colloids Surf. A: Physicochem. Eng. Aspects 254 (2005) 99.
[15] Y.S. Song, D.Y. Lee, B.Y. Kim, Effect of glass frit addition on corrosion resistance of Ti/TiO_2/IrO_2–RuO_2 films, Mater. Lett. 58 (2004) 817.

[16] A.F. Caliman, C. Cojocaru, A. Antoniadis, I. Poulios, Optimized photocatalytic degradation of Alcian Blue 8 GX in the presence of TiO_2 suspensions, J. Hazard. Mater. 144 (2007) 265.
[17] R.D. Cook, Residuals and Influence in Regression, Chapman and Hall, New York, 1982.
[18] G.E.P. Box, D.R. Cox, An analysis of transformations, J. Roy. Stat. Soc. B26 (1964) 211.
[19] M.N. Chong, S. Lei, B. Jin, C. Saint, C. Chow, Optimisation of an annular photoreactor process for degradation of Congo Red using a newly synthesized titania impregnated kaolinite nano-photocatalyst, Sep. Purif. Technol. , in press, doi:10.1016/j.seppur.2009.04.001.
[20] E. Sayan, M. Bayramoglu, Statistical modelling of sulphuric acid leaching of TiO_2 from red mud, Hydrometallurgy 57 (2000) 181.